A modeling of the magnetic levitation stage and its control

Taek-Kun Nam*, Yong-Joo Kim*, Jeong-Woo Jeon* , and Ki-Chang Lee*

* Machine control and application group, Korea Electrotechnology Research Institute, Korea
(Tel : +82-55-280-1541; E-mail:tknam@keri.re.kr, yjkim@keri.re.kr, jwjeon@keri.re.kr, leekc@keri.re.kr)

Abstract: In this paper, we address the development of magnetic levitation positioning system. This planar magnetic levitator employs four permanent magnet liner motors. Each motor generates vertical force for suspension against gravity, as well as horizontal force for drive levitation object called a platen This stage can generate six degrees of freedom motion by the vertical and horizontal force. We derived the mechanical dynamics equation using lagrangian method and used coenergy to express an electromagnetic force. We proposed control algorithm for the position and posture control from its initial value to its desired value using sliding mode control. Some simulation result is provided to verify the effectiveness of the proposed control scheme.

Keywords: magnetic levitation, lagrangian, coenergy, sliding mode control

1. INTRODUCTION

The importance of high precision positioning mechanism is increased with the high demand of advanced technologies delivering products with superior performance and good tolerance. We can easily found that high precision positioning mechanisms have play an important role in the field of modern fabrication process such as ultra precision machining, precise alignment of optical device, and wafer steppers in semiconductor manufacturing. Such devices could be support micro or even nano positioning accuracy, high bandwidths of operation, and sufficient stiffness. Piezoelectric actuators provide the necessary stiffness and positioning accuracy but have some restriction with its traveling range. Utilization of mechanical bearings or cascading arrangements suffer from slow speed of response and the presence of undesirable mechanical elements, such as clearances and friction. The combination of linear motor and air-bearing is a general strategy to realize long stroke movement with high velocities. But to achieve a large and accurate travel in multiple degrees of freedom using linear motor with non-contact bearing, it needs complex system configuration. In contrast, the magnetic levitation is contact-less mechanism which enabling high precision positioning accuracy and multiple d.o.f (degrees of freedom) could be achieved without mechanical guide or compounding.

In the previous works for the control of magnetic levitation positioner, Cho[3] tackled position control of magnetic suspension actuator with one d.o.f using sliding mode control method. Mittal [9] addressed long travel motion control of a magnetic suspension actuator using a combination of feedback linearization technique and discrete-time delay compensation algorithm. Kim et al. developed magnetic levitation stage with a six degree of freedom(6 DOF) [6]. Holmes modified the stage to develop a long range scanning stage and achieved sub-nanometer resolution [8].

We designed magnetic levitation stage as inferred the result of Kim [6]. The differences between Kim [6] and our work are as follows. A linear approximation and lead-lag compensator was applied to control the magnetic levitation stage [6]. In our work, we derived mechanical dynamics equation of the platen using Lagrangian equation and proposed configuration control algorithm using sliding mode control method. The sliding mode control method can be applied to a nonlinear system in the global sense, and the performance and stability robustness to model uncertainty and disturbances could be achieved by control switching. Finally, we verified the effectiveness of the proposed control scheme from a numerical simulation.

2. MAGNETIC LEVITATION STAGE

2.1 System Configuration

Magnetic levitation stage is as shown in Fig. 1. This levitator composed by four permanent magnet linear motors. Each motor generates vertical force for suspension against gravity and horizontal force for drive. The actuators for this magnetic levitator are three phase surface-wound surface-permanent –magnet linear motors.

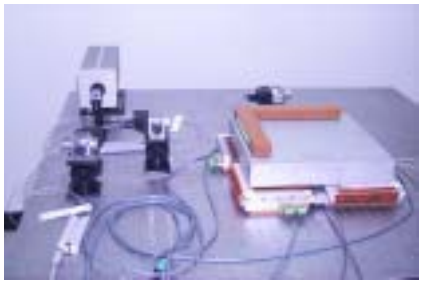

Fig. 1. Magnetic levitation stage.

The configuration of stage system is as shown in Fig. 2. The plane displacements of platen can be measured by three laser interferometers with sub-nanometer resolution and three capacitance probes adapted for the measurement of levitation gap and rotation angles. The desired command calculated on the control algorithm will be transferred to D/A signal to generate suitable current input.

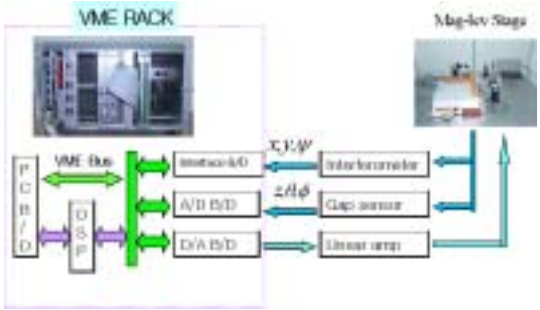

Fig. 2. Configuration of system.

3. CONTROL

3.1 Mechanical System Modeling

In this section, we will derive the dynamics equation of the magnetic levitation stage. The coordinates of platen which is the levitation part of the stage is shown in Fig. 3.

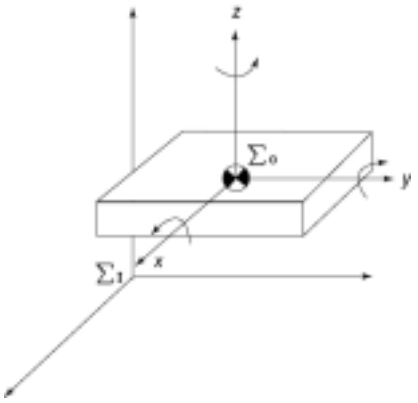

Fig. 3. Coordinates of the platen.

In the figure, Σ_I and Σ_O represent inertial coordinates frame and object coordinates frame, respectively.

Here $\eta_1 = [x, y, z]^T$, $\eta_2 = [\phi, \theta, \psi]^T$ denotes the position and orientation vector with coordinates in the inertial coordinates frame, $v_1 = [u, v, w]^T$, $v_2 = [p, q, r]^T$ denotes the linear and angular velocity vector with coordinates in the object coordinate frame.

The platen's movement path relative to the inertial frame is given by a velocity transformation

$$\dot{\eta}_1 = J_1(\eta_2) v_1 \tag{1}$$

$$J_1(\eta_2) = \begin{pmatrix} c\psi c\theta & -s\psi c\phi + c\psi s\theta s\phi & s\psi s\phi + c\psi c\phi s\theta \\ s\psi c\theta & c\psi c\phi + s\psi s\theta s\phi & -c\psi s\phi + s\psi c\phi s\theta \\ -s\theta & c\theta s\phi & c\theta c\phi \end{pmatrix}$$

where J_1 is a transformation matrix which is related through the functions of the Euler angles: ψ (yaw), θ (pitch), ϕ (roll). The inverse velocity transformation can be written

$$v_1 = J_1^{-1} \dot{\eta}_1 \tag{2}$$

where J_1 is skew-symmetric matrix, i.e. $J_1(\eta_2)^{-1} = J_1(\eta_2)^T$.

The object-fixed angular velocity vector $v_2 = [p\ q\ r]^T$ and the Euler rate vector $\dot{\eta}_2$ are related through a transformation matrix J_2 according to

$$v_2 = J_2^{-1}(\eta_2) \dot{\eta}_2 \tag{3}$$

It should be noted that the angular velocity vector v_2 cannot be integrated directly to obtain actual angular coordinates. The orientation of the object-fixed reference frame with respect to the inertial frame is given by

$$v_2 = \begin{pmatrix} \dot{\phi} \\ 0 \\ 0 \end{pmatrix} + C_{x,\phi} \begin{pmatrix} 0 \\ \dot{\theta} \\ 0 \end{pmatrix} + C_{x,\phi} C_{y,\theta} \begin{pmatrix} 0 \\ 0 \\ \dot{\psi} \end{pmatrix} \tag{4}$$

$$= \begin{pmatrix} 1 & 0 & -s\theta \\ 0 & c\phi & c\theta s\phi \\ 0 & -s\phi & c\theta c\phi \end{pmatrix} \dot{\eta}_2$$

From the above relations, we can formulate a suitable expression for the platen's kinetic energy

$$\begin{aligned} \mathrm{T} &= \frac{1}{2} m v_1^T v_1 + \frac{1}{2} v_2^T H v_2 \\ &= \frac{1}{2} m \dot{\eta}_1^T \dot{\eta}_1 + \frac{1}{2} \dot{\eta}_2^T J_2^{-T} H J_2^{-1} \dot{\eta}_2 \end{aligned} \tag{5}$$

and potential energy

$$V = mgz \tag{6}$$

Then we can compute the lagrangian L according to

$$L = T - V \tag{7}$$

Finally, applying the lagrange equation

$$\frac{d}{dt}\left(\frac{\partial L}{\partial \dot{q}}\right) - \frac{\partial L}{\partial q} = u \tag{8}$$

We can get dynamics equation

$$M\ \ddot{q} + h_1 + h_2(q, \dot{q}) = u \tag{9}$$

$q = [x, y, z, \psi, \theta, \phi]^T$ is a state variables that represent the motion of system. $u = [F\ \tau]^T$ is input vector which denotes forces and moments acting on the platen in the object-fixed frame. $M \in R^{6\times 6}$ is an inertia matrix.

3.2 Electrical System Modeling

In this section we will consider an electrical dynamics for the levitation stage. Electrical dynamics can be derived from the Faraday's law. The voltage equations of three phase motor can be written

$$R_k i_k + \frac{d\lambda_k}{dt} = v_k, k = 1,2,3. \tag{10}$$

where R_k is the resistance of winding and λ_k is the flux linkage of each phase winding. We can represent λ_k

$$\lambda_k(i_k, x, y, z) = \lambda_k(i_k, x - l, y, z) \tag{11}$$

We know that the flux linkage is periodic function with respect to x direction. Using chain-rule, we can get voltage equations as

$$R_k i_k + L_k(i_k, x, y, z)\frac{di_k}{dt} + E_{kx} + E_{ky} + E_{kz} = v_k \tag{12}$$

where

$$L_k = \frac{\partial \lambda_k}{\partial i_k},\ E_{kx} = \frac{\partial \lambda_k}{\partial x}\dot{x},\ E_{ky} = \frac{\partial \lambda_k}{\partial y}\dot{y},\ E_{kz} = \frac{\partial \lambda_k}{\partial z}\dot{z} \tag{13}$$

It is well known that coenergy is convenient quantity for expressing the electromagnetic force. We will introduce the coenergy to derive the electromagnetic force generated by the

current input. Derivative of co-energy can be defined

$$dW_c = \sum_{k=1}^{3} \lambda_k di_k + f_x dx + f_y dy + f_z dz \quad (14)$$

Integrating eq. (14) from $(0,0,0,0,0,0)$ to (i_1, i_2, i_3, x, y, z), then we can get

$$W_c = \sum_{k=1}^{3} \int_0^{i_k} \lambda_k(\eta, x, y, z) d\eta \quad (15)$$

Applying the chain-rule to eq. (15) and comparing with eq. (14), we have

$$\begin{aligned} &\lambda_k(i_k, x, y, z) = D_k W_c(i_1, i_2, i_3, x, y, z), k = 1,2,3 \\ &f_x(i_1, i_2, i_3, x, y, z) = D_4 W_c(i_1, i_2, i_3, x, y, z) \\ &f_y(i_1, i_2, i_3, x, y, z) = D_5 W_c(i_1, i_2, i_3, x, y, z) \\ &f_z(i_1, i_2, i_3, x, y, z) = D_6 W_c(i_1, i_2, i_3, x, y, z) \end{aligned} \quad (16)$$

where D_k reveals k th partial differentiator.

Therefore, generating force f_x, f_y, f_z which has $2\pi/3$ phase difference can be obtained

$$\begin{aligned} f_x(i_1, i_2, i_3) &= \sum_{k=1}^{3} F_{xe}(i_k, x - \frac{l}{3}(k-1), y, z) \\ f_y(i_1, i_2, i_3) &= \sum_{k=1}^{3} F_{ye}(i_k, x - \frac{l}{3}(k-1), y, z) \\ f_z(i_1, i_2, i_3) &= \sum_{k=1}^{3} F_{ze}(i_k, x - \frac{l}{3}(k-1), y, z) \end{aligned} \quad (17)$$

where F_{xe}, F_{ye}, F_{ze} are

$$\begin{aligned} F_{xe} &= \int_0^i D_4 \lambda(\eta, x, y, z) d\eta \\ F_{ye} &= \int_0^i D_5 \lambda(\eta, x, y, z) d\eta \\ F_{ze} &= \int_0^i D_6 \lambda(\eta, x, y, z) d\eta \end{aligned} \quad (18)$$

Now we will consider flux linkage λ. Flux linkage can be written

$$\lambda(i, x, y, z) = \lambda_m(x, y, z) + \lambda_r(i, x, y, z) \quad (19)$$

where λ_m and λ_r reveals flux linkage generated by magnet array and current input into the stator, respectively. The flux linkage λ_m decreased by increasing the height of platen and changed with respect to x direction. Then we have

$$\lambda_m(x, y, z) = \alpha(z)\lambda_a(x), 0 < \alpha(z) \le 1 \quad (20)$$

where $\alpha(z)$ is monotone decreasing function and $\lambda_a(x)$ is a periodic function with respect to x axis.

The flux linkage λ_r can be represented

$$\lambda_r(x, y, z) = L(z)i \quad (21)$$

since the inductance L is only influenced by the height of platen.

Now we can calculate E_x, E_y, E_z in eq. (12)

$$\begin{aligned} E_x(i, x, \dot{x}, y, z) &= \dot{x}\alpha(z) g_a(x) \\ E_y(i, x, y, \dot{y}, z) &= 0 \\ E_z(i, x, y, z, \dot{z}) &= \dot{z}[\frac{d\alpha(z)}{dz}\lambda_a(x) + \frac{dL(z)}{dz} i] \end{aligned} \quad (22)$$

where g_a denotes $\frac{d\lambda_a(x)}{dx}$.

Substituting eq. (22) into eq. (12), we have

$$\begin{aligned} L(z)\frac{di_k}{dt} = -Ri_k - \dot{z}[&\frac{d\alpha(z)}{dz}(\lambda_a(x) + \lambda_b(y)) + \\ &\frac{dL(z)}{dz} i] - \dot{x}\alpha(z) g_a(x) - \dot{y}\alpha(z) g_b(y) + v_k \end{aligned} \quad (23)$$

Forces generated by current input will be

$$\begin{aligned} f_x &= \sum_{k=1}^{3} \alpha(z) g_a(x - \frac{l}{3}(k-1)) i_k \\ f_z &= \sum_{k=1}^{3} [\frac{d\alpha(z)}{dz}\lambda_a(x - \frac{l}{3}(k-1)) i_k + \frac{1}{2}\frac{dL(z)}{dz} i_k^2] \end{aligned} \quad (24)$$

We applied d-q transformation to eq. (23) and eq.(24). The d-q transformation was introduced to separate the stator current component that generates torque. Then, force equations and commutation in d-q frame do not contain the position dependence with respect to the stator. Therefore, nonlinearity due to the trigometric function in the model can be eliminated. Fig. 4 depicts d-q frame attached on the platen[6].

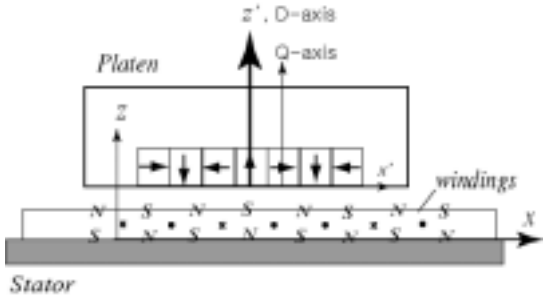

Fig. 4. d-q frame attached to the platen.

It is shown that the q axis is orthogonal to the d axis and leads it by 90^o. Applying d-q transformation, we have voltage equations on d-q axis from eq. (23)

$$\begin{aligned} L(z)\frac{di_d}{dt} &= v_d - Ri_d - \dot{z}(\frac{d\alpha(z)}{dz}\lambda_{d1}(x) + \frac{dL(z)}{dz} i_d) - \\ &\dot{x}\alpha(z) g_{d1}(x) + \frac{2\pi}{i} L(z)\dot{x} i_q \\ L(z)\frac{di_q}{dt} &= v_q - Ri_q - \dot{z}(\frac{d\alpha(z)}{dz}\lambda_{q1}(x) + \frac{dL(z)}{dz} i_q) - \\ &\dot{x}\alpha(z) g_{q1}(x) + \frac{2\pi}{i} L(z)\dot{x} i_d \end{aligned} \quad (25)$$

Forces f_x, f_z can be calculated

$$f_x = \frac{3}{2}[\frac{d\alpha(z)}{dz}\lambda_{d1}(x)i_d + \frac{d\alpha(z)}{dz}\lambda_{q1}(x)i_q] + \frac{3}{4}\frac{dL(z)}{dz}(i_d^2 + i_q^2) \quad (26)$$

$$f_z = \frac{3}{2}\alpha(z)[g_{d1}(x)i_d + \alpha(z)g_{q1}(x)i_q]$$

3.3 The relations between forces and torque

Each motor generates vertical force for suspension against gravity, as well as horizontal force for drive a platen. Therefore, this stage can generate six degrees of freedom motion by the vertical and horizontal force. The relations between d.o.f and generating forces can be verified as shown in Fig. 5.

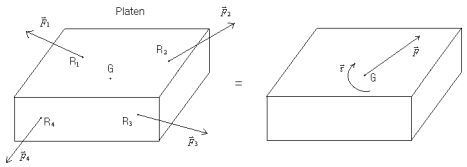

Fig. 5. The relation between forces and torque on the platen.

The horizontal forces can be represented

$$F = \sum_{i=1}^{4}\vec{F}_i = \begin{bmatrix} F_X \\ F_Y \\ F_Z \end{bmatrix} = \begin{bmatrix} f_{1x} + f_{3x} \\ f_{2y} + f_{4y} \\ \sum_{i=1}^{4} f_{iz} \end{bmatrix}_{XYZ} \quad (27)$$

where $[]_{XYZ}$ denotes inertial coordinates frame. The torques on the center of the mass of the platen will be

$$\vec{\tau} = \begin{bmatrix} \tau_X \\ \tau_Y \\ \tau_Z \end{bmatrix} = \sum_{i=1}^{4}\tau_i = \begin{bmatrix} b_1 f_{1z} + b_2 f_{2z} + b_3 f_{3z} + b_4 f_{4z} - c_2 f_{2y} - c_4 f_{4y} \\ c_1 f_{1z} + c_3 f_{3z} - a_1 f_{1z} - a_2 f_{2z} - a_3 f_{3z} - a_4 f_{4z} \\ a_2 f_{2y} + a_4 f_{4y} - b_1 f_{1x} - b_3 f_{3x} \end{bmatrix} \quad (28)$$

where $[a_i, b_i, c_i]^T$ reveals the displacement vectors from the center of mass of the platen to the center of mass of each of four magnet array

$$\begin{bmatrix} a_i \\ b_i \\ c_i \end{bmatrix} = (J_1)^{-1}\begin{bmatrix} x_i \\ y_i \\ z_i \end{bmatrix}_{x'y'z'} \quad (29)$$

Finally, we can compile the relation between forces and torque on the platen

$$\begin{bmatrix} F_X \\ F_Y \\ F_Z \\ \tau_X \\ \tau_Y \\ \tau_Z \end{bmatrix} = \begin{bmatrix} 1 & 0 & 0 & 0 & 1 & 0 & 0 & 0 \\ 0 & 0 & 1 & 0 & 0 & 0 & 1 & 0 \\ 0 & 1 & 0 & 1 & 0 & 1 & 0 & 1 \\ 0 & b_1 & -c_2 & b_2 & 0 & b_3 & -c_4 & b_4 \\ c_1 & -a_1 & 0 & -a_2 & c_3 & -a_3 & 0 & -a_4 \\ -b_1 & 0 & a_2 & 0 & -b_3 & 0 & -a_4 & 0 \end{bmatrix}\begin{bmatrix} f_{1x} \\ f_{1z} \\ f_{2x} \\ f_{2z} \\ f_{3x} \\ f_{3z} \\ f_{4x} \\ f_{4z} \end{bmatrix} \quad (30)$$

3.4 Control Strategy

Based on the mechanical and electrical dynamics equation, we can design the control input to achieve desired movement of platen. The procedure to design control algorithm is as follows.

- To design control forces and torques (F, τ) in eq. (9) to move the platen from its initial posture to its desired one.
- Calculate desired forces($f_{1x} \sim f_{4z}$) on the stator from eq. (30).
- Using eq. (26), we can get the desired current i_d, i_q which can generate desired forces in the second step.
- After calculating desired voltage v_d, v_q from eq. (25), then we have 3 phase input voltage using d-q inverse transformation.

In this section, we will propose the control algorithm which is needed in the first step. Here we consider sliding mode control method which maintains robustness in the presence of a model uncertainty and external disturbance.

Consider inertia matrix in (6) as

$$M = M^0 + \Delta M \quad (31)$$

where, M^0 denotes estimated value and ΔM represents an error value between real value and estimated value.

Let us assume each components of the inertia matrix can be estimate its maximum value

$$|\Delta M_{ij}(q)| \le \hat{M}_{ij} \quad (32)$$

To compensate the gravity terms, we introduce control input

$$u = v + h_1 \quad (33)$$

where v denotes new control input and h_1 is a gravity compensation term.

Substituting (7) and (9) into (6), then we have

$$\ddot{q} = M^{0^{-1}}(v + d) \quad (34)$$

$d(q, \dot{q}, \ddot{q}) = -\Delta M\dot{q} - h_2$ denotes an estimated error and nonlinear terms of the dynamics equation. We assume d can be estimated by scalar function $\hat{d}(q,t)$

$$|d| \le \hat{d} \quad (35)$$

To achieve tracking performance, define the tracking errors as

$$e(t) = q - q_r, \ \dot{e}(t) = \dot{q} - \dot{q}_r \quad (36)$$

where, q and q_r denote current state variable and desired state variable, respectively.

Here we introduce switching surface

$$\sigma(t) = \dot{e} + \Lambda e$$
$$\Lambda = diag(\lambda_1, \cdots, \lambda_n) \quad (37)$$

From eq. (37), we can see that $\sigma(t) \to 0$ means stabilization of error variable e because it makes stable error equation $\dot{e} = -\Lambda e$. The control problem is to derive control input u which guarantees $\sigma(t) \to 0$ and preserve states $q, \dot{q}$ on the sliding surface. To derive such a control input, we

can consider Lyapunov function candidates

$$V = \frac{1}{2}\sigma^T\sigma \tag{38}$$

Time differentiation of eq. (38) is

$$\begin{aligned}\dot{V} &= \sigma^T\dot{\sigma} \\ &= \sigma^T(\ddot{e} + \Lambda\dot{e}) \\ &= \sigma^T(M^{0^{-1}}v + M^{0^{-1}}d - \ddot{q}_r + \Lambda\dot{e})\end{aligned} \tag{39}$$

Considering new control input as

$$v = M^0(\ddot{q}_r - \Lambda\dot{e} - K\frac{\sigma}{\|\sigma\|}) \tag{40}$$

where, $K > \|M^0\| \cdot \hat{d}$

Then, we have

$$\dot{V} = -\|\sigma\|(K \pm M^0 d) \le 0 \tag{41}$$

Therefore, $\sigma(t) \to 0, t \to \infty$ was achieved by control input (40). The control input to achieve configuration control purpose can be obtained from eq. (33) and eq. (40)

$$u = M^0(\ddot{q}_r - \Lambda\dot{e} - K\frac{\sigma}{\|\sigma\|}) + h_1 \tag{42}$$

3.5 Simulation Result

To illustrate the effectiveness of the proposed control scheme, we present a simulation result for an magnetic levitation stage. In the simulation, initial value q_0 and desired value q_r are $(0,0,250\mu m,0.1,0.2,0.3,0,0,0,0,0,0)^T$ and $(0,0,350\mu m,0,0,0,0,0,0,0,0,0)^T$, respectively. We set the parameters as $m = 5.47[kg]$, $g = 9.8[m/s^2]$, $\Lambda = diag[3,3,3,3,3,3]$. Estimated value M^0 was considered to 40% of the real value. In the simulation we introduced smoothing function $u = M^0(\ddot{q}_r - \Lambda\dot{e} - K\frac{\sigma}{\|\sigma\| + \delta}) + h_1$, $\delta > 0$ to decrease chattering phenomenon . The numerical simulation result for the configuration control is shown in Fig. 6. Fig. 6(a) and Fig. 6(b) show the time evolution of state variables. Fig. 6(c) and Fig. 6(d) depict control input generated by proposed control strategy.

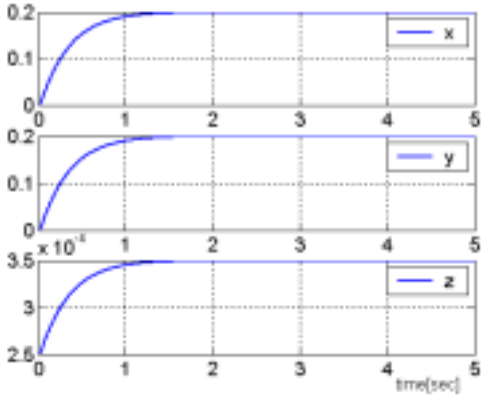

Fig. 6(a). Time evolution of states: x, y, z.

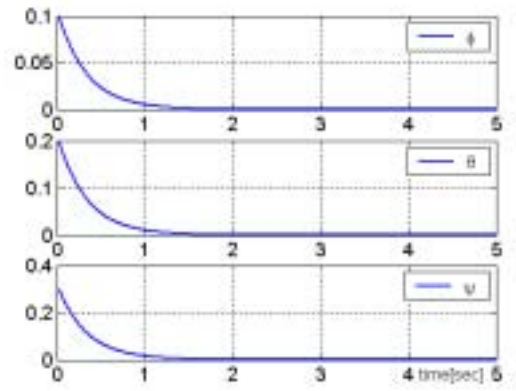

Fig. 6(b). Time evolution of states: ϕ, θ, ψ .

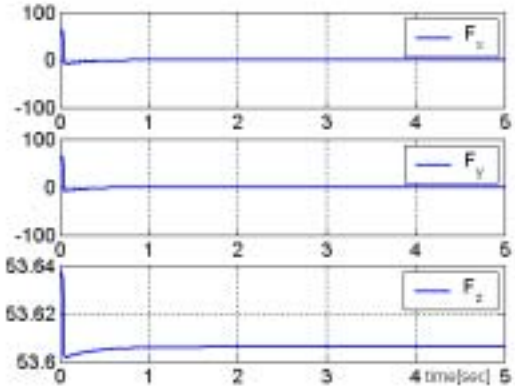

Fig. 6(c). Time evolution of control inputs: f_x, f_y, f_z.

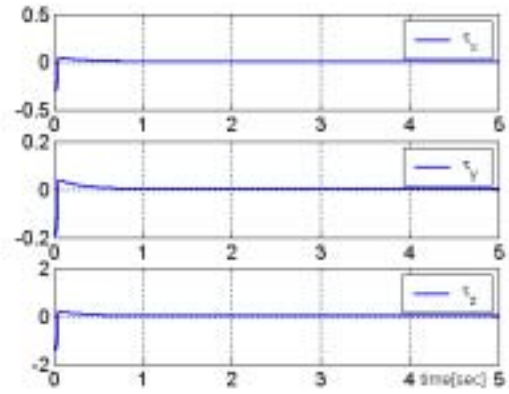

Fig. 6(d). Time evolution of control inputs: τ_x, τ_y, τ_z .

From the above result, we see that control purpose was achieved by proposed control algorithm.

4. CONCLUSIONS

In this paper, we addressed configuration control for the magnetic levitation stage. We derived dynamic equation of the platen and proposed control strategy which can control its position and posture. To derive control input, we applied sliding mode control method which can be maintain the performance and stability robustness to model uncertainty and disturbances. Finally, We verified an effectiveness of the control algorithm by numerical simulation.

REFERENCES

[1] V.I.Utkin, "Variable structure systems with sliding mode", IEEE Trans. Automation and Control, vol. AC-22, pp. 212-222, 1977.

[2] S.C. Fawcett, " Small amplitude vibration compensation for precision diamond turning", *Precision turning* vol. 12, no. 2, pp. 91-96, 1990.

[3] M.Y.Chen, M.J.Wang, and L.C.Fu, "A Novel dual axis repulsive maglev guiding system with permanent magnet: modeling and controller design", IEEE/ASME Trans. on mechatronics, vol. 8, no. 1, pp. 77-86, 2003.

[4] D.Cho, Y.Kato and D.Spilman, "Sliding mode and classical controller in magnetic levitation," IEEE control sytems, pp. 42-48 , 1993.

[5] R. Nicole, Title of paper with only first word capitalized," *J. Name Stand. Abbrev.*, in press.

[6] W.J.Kim, "High-Precision planar magnetic levitation", Ph. D. Dissertation, Massachusetts Institute of Technology, 1997.

[7] W.J.Kim, D.L. Trumper, "High-Precision planar magnetic levitation stage for photolithograpy", *Precision Engineering*, vol. 22, no.2, pp. 66-77, 1998.

[8] M.L.Holmes, R.Hocken and D.L. Trumper, "The long range scanning stage: a novel platform for scanned probe microscopy", *Precision Engineering*, vol. 24, no.3, pp. 191-209, 2000.

[9] S.Mittal, C.H.Menq, "Precision motion control of a magnetic suspension actuator using a robust nonlinear compensation scheme", *IEEE/ASME Tran. on Mechatronics*, vol. 2, no. 4, pp. 268-280, 1997.

[10] K.Park et al., "Magnetic levitated high precision positioning system based on antagonistic mechanism", *IEEE Tran. on Magnetics*, vol. 32, pp. 208-219, 1996.